FORCE FEEDBACK VERSUS ACCELERATION FEEDBACK IN ACTIVE VIBRATION ISOLATION

A. Preumont, A. Francois, F. Bossens and A. Abu-Hanieh

Active Structures Laboratory, Université Libre de Bruxelles,
CP. 165-42, 50 Av. F.D. Roosevelt, B-1050 Brussels, Belgium
e-mail: andre.preumont@ulb.ac.be

ABSTRACT

This note compares the force feedback and acceleration feedback implementation of the sky-hook damper when it is used to isolate a flexible structure from a disturbance source. It is shown that the use of a force sensor produces always alternating poles and zeros in the open-loop transfer function between the force actuator and the force sensor, which guarantees the stability of the closed-loop. On the contrary, the acceleration feedback produces alternating poles and zeros only when the flexible structure is stiff compared to the isolation system; this property is lost when the flexible modes of the sensitive payload interfere with the isolation system.

1. INTRODUCTION

Vibration isolation is concerned with the development of an interface between a vibration source and a vibration-sensitive equipment, which attenuates the vibration transmission above the corner frequency of the isolation system [1]. As an example, a precision payload (such as a telescope) must be isolated to be protected from the jitter induced by the reaction wheel assembly of the attitude control system of a spacecraft [2]. On the other hand, the isolation system must allow the low frequency attitude control torque to be transmitted to the spacecraft.

Any passive isolation system consists of one or several stages of springs and dampers introduced in the vibration propagation path; their parameters are adjusted to achieve a desired corner frequency and a reasonable compromise between the amplification at the resonances and the high frequency attenuation. The passive damping is necessary to limit the amplification at resonance, but it tends to reduce the high frequency attenuation of the isolation system.

Active vibration isolation aims at improving the performance of the vibration isolation by including a force generating element in the isolation interface, a sensor at the receiving end of the transmission path, and a feedback control law connecting them. The celebrated *sky-hook* damper [3, 4] is a single stage interface which allows to combine a -40 dB/decade attenuation rate at high frequency with a critical damping (no overshoot) at resonance.

Section 2 reviews the sky-hook damper for the single d.o.f. isolator connecting two rigid bodies; it also discusses two sensing options (namely acceleration of the sensitive payload and the total force transmitted by the isolator). Next, the paper compares the two sensing options when the sensitive equipment is flexible, which is more representative of a large space structure; in section 3 a two d.o.f. sensitive equipment is considered. In section 4, a general result is established, which guarantees the interlacing of the poles and zeros for a force feedback.

Section 5 considers a free free beam to illustrate the superiority of the force feedback option over the acceleration feedback when the flexible modes of the sensitive payload interfere with the isolation system.

2. SKY-HOOK DAMPER

Consider the single-axis isolator connecting two rigid bodies as in Fig.1 (x_d and m are the displacement and mass of the disturbance source, x_c and M are the displacement and mass of the sensitive equipment, s is the Laplace variable, g is the control gain, $X_c(s)$ is the Laplace transform of x_c, sX_c is the Laplace transform of $\dot{x}_c$, etc ...). The classical implementation of the sky-hook damper is that of Fig.1.a: an acceleration sensor is placed on the sensitive equipment, measuring its absolute acceleration $\ddot{x}_c$ (or s^2X_c); the sensor signal is passed through an integral controller ($-g/s$) leading to a control force proportional to the absolute velocity of the sensitive equipment, $F_a = -gsX_c$. The name *sky-hook damper* comes from the fact that this force could conceptually be achieved with a passive damper connecting the sensitive equipment to a fixed point in space (the sky, Fig.1.b). Since the force applied to a rigid body is proportional to its acceleration, the feedback based on the acceleration $\ddot{x}_c$ of the sensitive equipment can alternatively be based on the sensing of the total interface force, $F = Ms^2X_c$ (Fig.1.c). The two control configurations are totally equivalent and they have the same open-loop transfer function :

$$G(s) = \frac{F(s)}{F_a(s)} = \frac{Ms^2X_c(s)}{F_a} = \frac{mMs^2}{mMs^2 + k(M+m)} \tag{1}$$
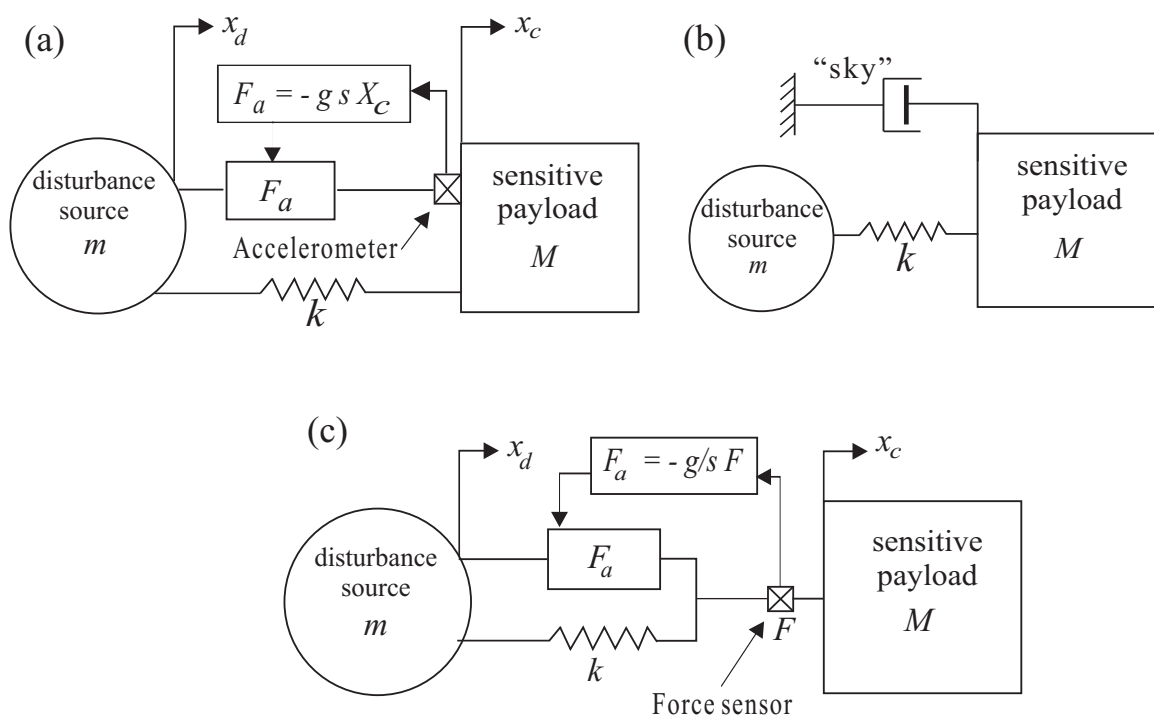

Figure 1: (a) Single axis soft isolator with acceleration feedback. (b) Equivalent "sky-hook" damper. (c) Force feedback isolator.
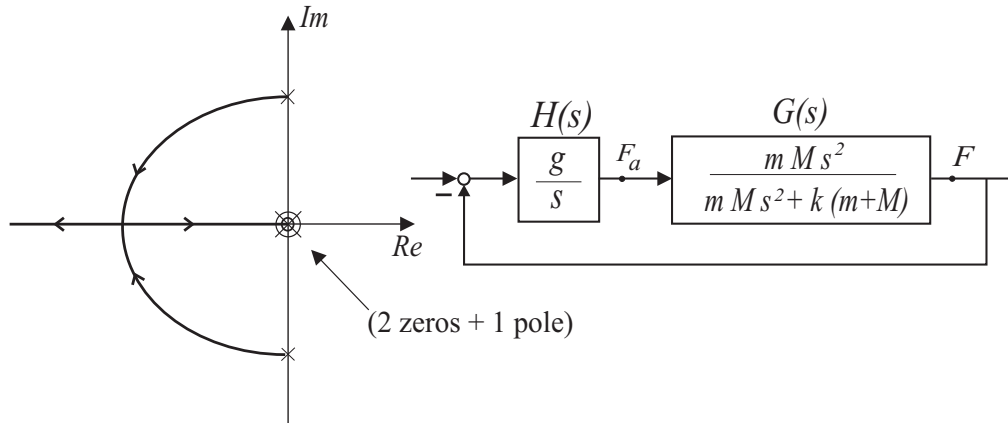
Figure 2: Root locus of the force feedback isolator connecting two rigid bodies

With the compensator $H(s) = g/s$, the characteristic equation of the closed-loop poles reads

$$1 + gH(s)G(s) = 1 + g\frac{s}{s^2 + \Omega^2} = 0 \tag{2}$$

where $\Omega^2 = \frac{k(M+m)}{mM}$ is the natural frequency of the two-mass system; the corresponding root locus is represented in Fig.2. The transmissibility of the force feedback isolator reads

$$\frac{X_c(s)}{X_d(s)} = \left[\frac{M}{k}s^2 + \frac{M}{k}gs + 1\right]^{-1} \tag{3}$$

which exhibits a -40 dB/decade attenuation rate at high frequency; the feedback gain g can be adjusted to achieve critical damping at the corner frequency.

We now examine the deviation between the two control strategies when the payload is flexible.

3. FLEXIBLE PAYLOAD

Next, we consider the situation where the sensitive payload is flexible as in Fig.3 (in the example of a spacecraft, the flexible appendage may represent a solar panel). The dynamics of the flexible payload is no longer governed by $F = ms^2 X_c$, so that the two sensing options are no longer equivalent. In fact, different sensor configurations correspond to different locations of the open loop transmission zeros in the complex plane. Before establishing a fairly general result on the stability of the force feedback, let us examine the simple example of Fig.3 with
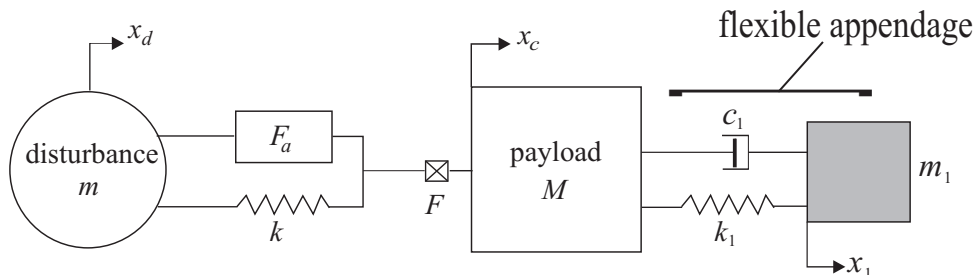

Figure 3: Payload with a flexible appendage.

the following numerical values: $m = 1.1kg$, $M = 1.7kg$, $k = k_1 = 12000N/m$, $c_1 = 0$ (assuming no damping, all the poles and zeros are on the imaginary axis); the mass m_1 of the flexible appendage is taken as a parameter to analyse the interaction between the flexibility of the payload and the isolation system. When m_1 is small, the frequencies of the additional pair of poles and zeros introduced by the flexible appendage are much higher than the isolator poles and the situation is not much different from that of a rigid body. As m_1 increases, they move along the imaginary axis towards the lower frequencies. Figure 4 shows the root locus plots for $m_1 = 0.5kg$; the acceleration feedback and the force feedback have similar root locus plots, with a new pole/zero pair appearing higher on the imaginary axis; the only difference between the two plots is the distance between the pole and the zero which is larger for the acceleration feedback; as a result, the acceleration feedback produces a larger damping of the higher mode. On the contrary, when m_1 is large, the root locus plots are reorganized as shown in Fig.5 for $m_1 = 3.5kg$. In the case of force feedback (Fig.5.a), the poles and zeros still alternate on the imaginary axis, leading to a stable root locus; this property is lost for the acceleration feedback (Fig.5.b), leading to an unstable loop for the lower mode. In practice, the presence of damping ($c_1 \neq 0$) moves this loop slightly to the left and allows to operate the control system for small gains, not enough, however to achieve critical damping on the suspension poles. Large space structures are usually very lightly damped. We now establish the central result of this paper.
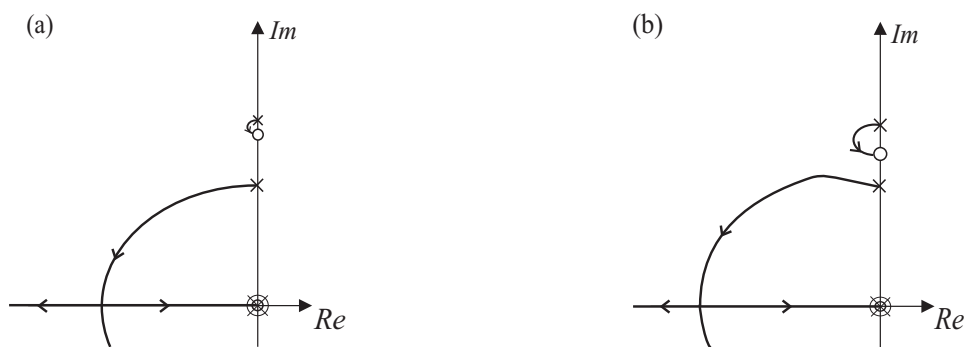

Figure 4: Root locus of the isolation system with a light flexible appendage ($m_1 = 0.5kg$). (a)Force feedback. (b)Acceleration feedback. (Only the upper half of the locus is shown)
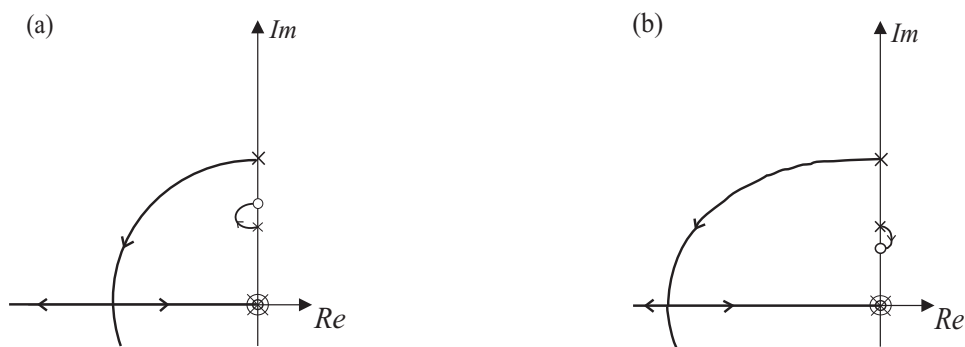

Figure 5: Root locus of the isolation system with a heavy flexible appendage ($m_1 = 3.5kg$). (a)Force feedback. (b)Acceleration feedback.
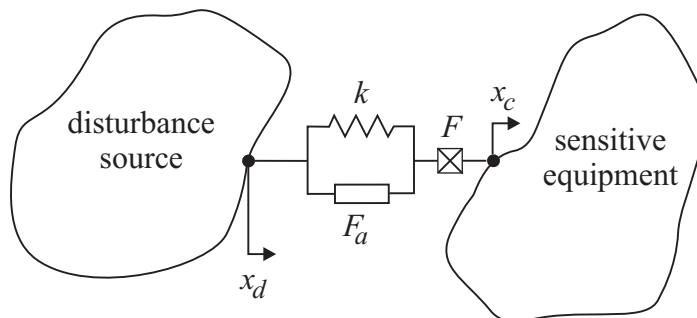
Figure 6: Two arbitrary flexible structures connected with a single axis soft isolator with force feedback.

4. OPEN-LOOP POLE/ZERO PATTERN OF A SOFT ISOLATOR WITH FORCE FEEDBACK

The following result confirms the observation of the previous example.

If two arbitrary flexible, undamped structures are connected with a single axis soft isolator with force feedback (Fig.6), the poles and zeros in the open loop transfer function $F(s)/F_a(s)$ alternate on the imaginary axis.

The proof stems from the property of the collocated systems with *energetically conjugated* input and output variables (e.g. force input and displacement output, or torque input and angle output): For such a system, all the residues in the modal expansion of the transfer function have the same sign and this results in alternating poles and zeros on the imaginary axis [5, 6].

If we now examine the transfer function between the control force F_a and the output of the force sensor F (Fig.6), although the actuator and sensor are collocated, F and F_a are not energetically conjugated and the preceding property does not apply. However, the total force F transmitted by the isolator is the sum of the control force F_a and the spring force, $k\Delta x$, where Δx is the relative displacement of the two structures along the isolator axis,

$$F = k\Delta x - F_a$$

or

$$\frac{F(s)}{F_a(s)} = k\frac{\Delta X(s)}{F_a(s)} - 1 \tag{4}$$

Thus, the open-loop transfer function F/F_a is the sum of $k\Delta X/F_a$ and a negative unit feedthrough. The input F_a and the output Δx involved in the transfer function $\Delta X/F_a$ are energetically conjugated and, as a result, the transfer function $\Delta X/F_a$ has all its residues positive and possesses alternating poles and zeros along the imaginary axis. The addition of a feedthrough term does not affect the residues in the modal expansion; the frequency response function (FRF) $F(\omega)/F_a(\omega)$ (obtained from the transfer function by setting $s = j\omega$, and which is purely real if the system is undamped) is obtained from the FRF $\Delta X(\omega)/F_a(\omega)$ by moving it along the ordinate axis by the amount of feedthrough; this changes the location of the zeros, without however changing the interlacing property (Fig.7). QED.
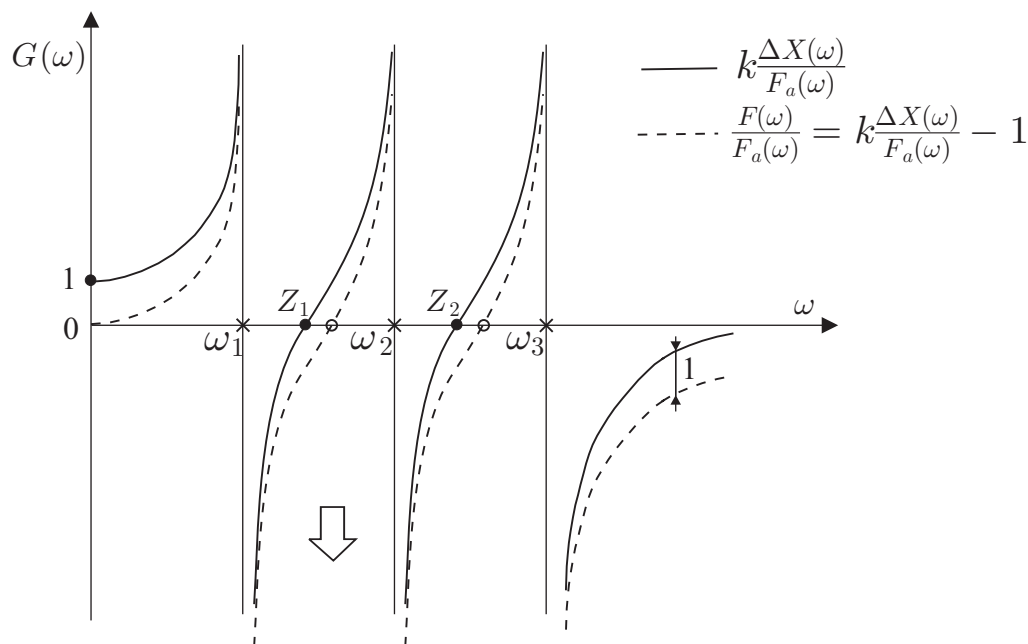
Figure 7: FRFs $k\frac{\Delta X(\omega)}{F_a(\omega)}$ and $\frac{F(\omega)}{F_a(\omega)}$ for an undamped structure (they are purely real). ω_i are the resonance frequencies and Z_i the transmission zeros. The unit feedthrough component which appears in F/F_a alters the location of the zeros (from ● to ○) without changing the interlacing property.

5. FREE-FREE BEAM

To illustrate further the influence of the sensing configuration on the pole/zero pattern, consider the free-free beam of Fig.8 with the following actuator/sensor configurations. This situation can be regarded as representative of a large space structure with its attitude control system (note that the rigid body modes are not controllable from the internal force F_a)

5.1. FREE-FREE BEAM ALONE

Consider the free-free beam of Fig.8.b with a force actuator (f) and a collocated acceleration sensor ($\ddot{y}$); the poles are $\pm j\Omega_i$ where Ω_i are the natural frequencies of the free-free modes of the beam. According to the physical interpretation of the zeros [7], they represent the resonances of the subsystem constrained by the sensor and the actuator. In this case, the constrained subsystem has an additional support as in the right side of Fig.8.b; the zeros are $\pm jZ_i$ where Z_i are the natural frequencies of the constrained system. Since the system is collocated and the input and output variables are energetically conjugated, the poles and zeros alternate on the imaginary axis:

$$Z_i < \Omega_i < Z_{i+1} \tag{5}$$

5.2. COMPLETE SYSTEM WITH FORCE SENSOR

Next consider the full system including the beam and the isolator with a force sensor (Fig.8.d). The poles are $\pm j\omega_i$, where ω_i are the natural frequencies of the global system (beam + isolator) while the transmission zeros are obtained as the resonances of the constrained subsystem, where the interface force between the isolator and the beam is constrained to be zero; this is equivalent to releasing the isolator from the beam, which means that the zeros
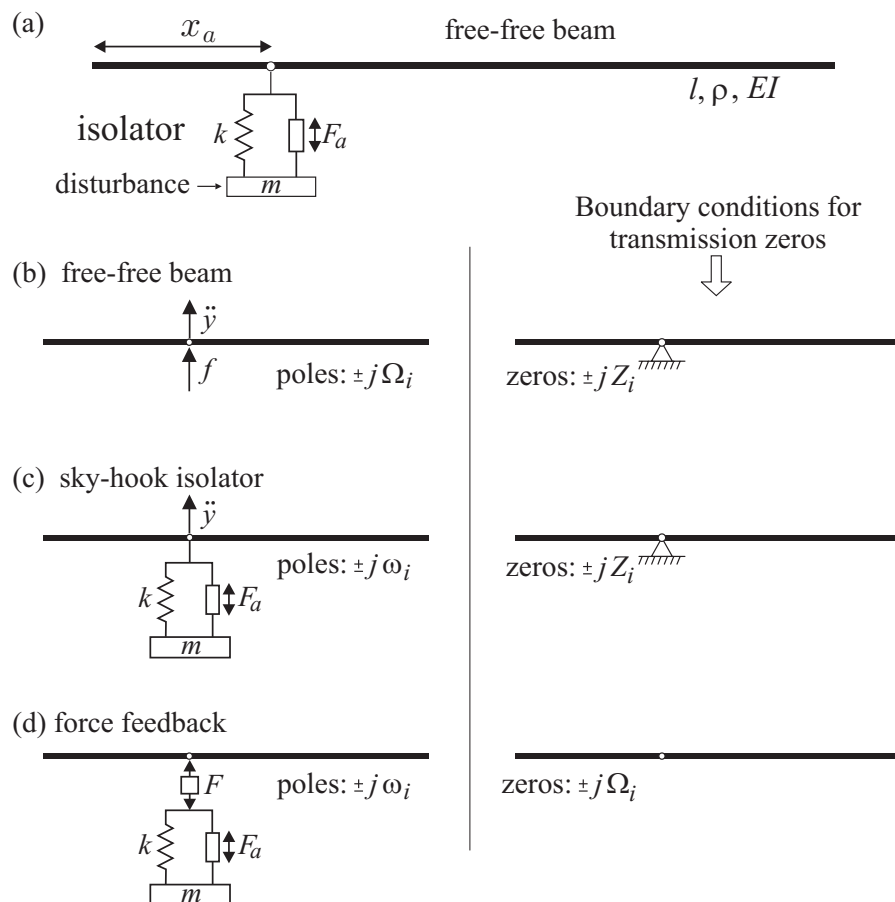
Figure 8: (a) Free-free beam and single axis isolator. The other figures illustrate the various situations and the boundary conditions corresponding to the transmission zeros. (b) Free-free beam alone with displacement sensor and point force actuator. (c) Free-free beam and sky-hook isolator (acceleration sensor). (d) Free-free beam and isolator with force feedback.

are $\pm j\Omega_i$ where Ω_i are the natural frequencies of the free-free beam (same as the poles for the configuration of Fig.8.b). We know from the previous section that the poles and the zeros also alternate in this configuration:

$$\omega_i < \Omega_i < \omega_{i+1} \tag{6}$$

5.3. COMPLETE SYSTEM WITH ACCELERATION SENSOR

This is the configuration of Fig.8.c, where an acceleration sensor has been substituted to the force sensor. The poles $\pm j\omega_i$ are the same as in the previous case (the poles do not depend on the sensor configuration) and the transmission zeros, corresponding to the resonances of the constrained subsystem where the acceleration of the connecting d.o.f. is zero, are $\pm jZ_i$, identical to those of Fig.8.b. No guarantee exist as to the interlacing of the poles and zeros for this sensor configuration, and it is easy to generate an example where this property is violated.

To illustrate this, Fig.9 shows the result of a numerical study performed with the numerical values given on the figure. The bending stiffness EI of the beam is taken as parameter. The figure shows the evolution of the poles (ω_i) and zeros (Ω_i and Z_i) of the various configurations
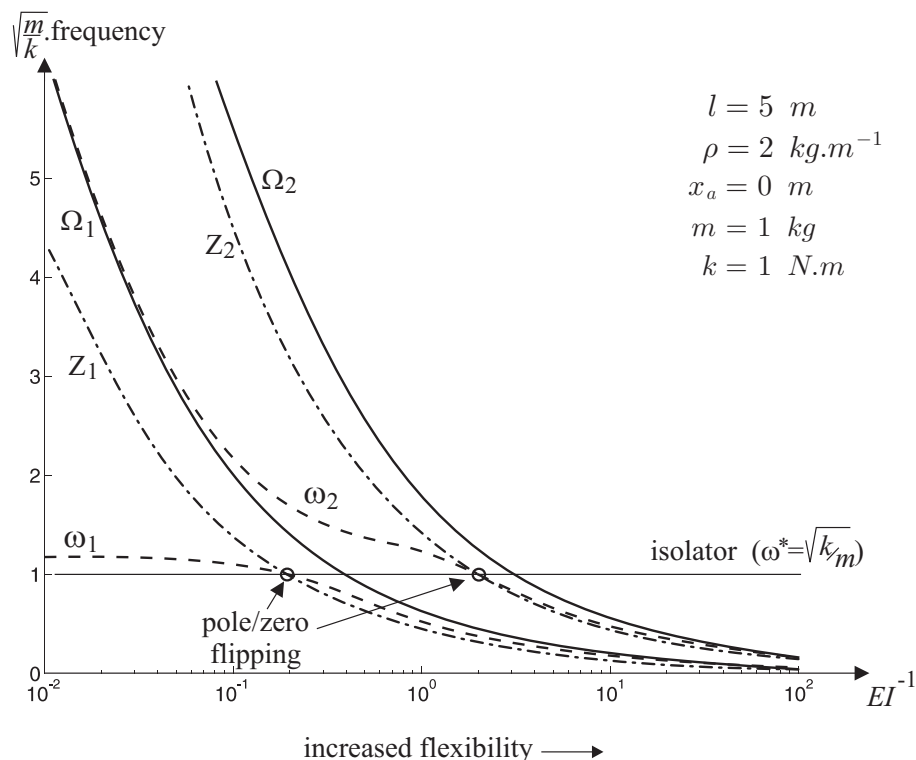
Figure 9: Flexible beam with an isolator; evolution of ω_i, Z_i and Ω_i with the flexibility of the beam.

as the flexibility of the beam increases (the frequency is made non-dimensional by dividing by the constrained natural frequency of the isolator, $\omega^* = \sqrt{k/m}$). The MATLAB simulation uses a truncated modal expansion (3 flexible modes) with the analytical mode shapes of the free-free beam, including a quasi-static correction for the high frequency modes (e.g. [6], ch.2).

As expected, the two interlacing properties (5) and (6) are always satisfied. When the beam is stiff, the interlacing property $\omega_i < Z_i < \omega_{i+1}$ is satisfied and the stability of the sky-hook damper is therefore guaranteed, but as the beam becomes more flexible, the values of ω_i and Z_i decrease at different rates and a pole/zero flipping occurs when they both become equal to the constrained frequency of the isolator, ω^*. Beyond this point the stability of the sky-hook damper is no longer guaranteed. This confirms the observations of the previous sections.

6. CONCLUSION

The sky-hook damper was originally developed with an acceleration measurement on the sensitive payload; an alternative implementation consists of measuring the total force transmitted across the isolator. The two strategies are totally equivalent in the case of a single axis isolator connecting two rigid bodies.

When the isolator connects flexible bodies, acceleration and force measurements are no longer equivalent. It has been shown that the use of a force sensor always produces alternating poles and zeros in the open-loop transfer function; this guarantees the stability of the closed-loop system in all circumstances. On the contrary, acceleration feedback does not exhibit alternating poles and zeros any longer when the flexible modes of the sensitive payload interfere with the isolation system.

7. ACKNOWLEDGMENT

REFERENCES

[1] C. Crede. *Vibration and Shock Isolation.* Wiley, 1986.

[2] R. A. Laskin and S. W. Sirlin. Future payload isolation and pointing system technology. *AIAA J. Guidance and Control*, 9(4):469–477, July–August 1986.

[3] D. C. Karnopp and A. K. Trikha. Comparative study of optimization techniques for shock and vibration isolation. *Trans. ASME, Journal of Engineering for Industry, series B*, 91(4):1128–1132, 1969.

[4] C. E. Kaplow and J. R. Velman. Active local vibration isolation applied to a flexible space telescope. *AIAA J. Guidance and Control*, 3(3):227–233, May–June 1980.

[5] G.D. Martin. *On the Control of Flexible Mechanical Systems.* PhD thesis, Stanford University, 1978.

[6] A. Preumont. *Vibration Control of Active Structures: An Introduction.* Kluwer, 1997. pp. 22-25.

[7] D. K. Miu. *Mechatronics.* Springer-Verlag, 1993. Chapter 8.